

# Unifying Indicator and Instantaneous Reaction Methods of Measuring Micromixing

Instantaneous chemical reactions, either themselves or together with chemical indicators, have previously been used as probes of turbulent micromixing. Both methods obtain statistics of the micromixing from measurement of time mean quantities. The mean reactant concentration, which is the quantity measured in the instantaneous reaction method, is shown here to be the integral with respect to feed concentration ratio of the mean color density, which is the quantity measured in the chemical indicator method. Differentiation of the mean color density gives the scalar probability density while integration gives the mean reactant concentration. Measurements of the color density of bromothymol blue at the centerline of a turbulent jet of base mixing with acid are used as an example.

U. V. Shenoy  
H. L. Toor

Department of Chemical Engineering  
Carnegie Mellon University  
Pittsburgh, PA 15213

## Introduction

Instantaneous chemical reactions, like acid-base neutralizations, are mixing controlled, and measurement of the conversion as a function of feed concentration ratio allows calculation of micromixing parameters like the scalar probability density function (PDF) and the intensity of segregation (or almost equivalent, the variance of the PDF), quantities of practical as well as theoretical interest (Kappel, 1979; Shenoy, 1988; Shenoy and Toor, 1989).

The same micromixing information can also be obtained by adding a chemical indicator to the system and measuring the mean color density of the indicator as a function of feed concentration ratio (Danckwerts, 1957; Li and Toor, 1986; Shenoy and Toor, 1988). When the measured mean is the time mean, local micromixing data are obtained. These two methods, the instantaneous reaction (IR) method, and the chemical indicator (CI) method, appear to have advantages over direct measurement with a passive tracer as they do not need probes which resolve fast transients. Thus the measurements are easier to make and are not limited by the inadequacies of instantaneous probes (Koochesfahani and Dimotakis, 1986).

In the IR method, conversion has been obtained by measuring the time mean temperature rise of the reaction and in this form the method is most easily applicable to one-dimensional systems where temperature rise and conversion are linearly related (Vassilatos and Toor, 1965; Mao and Toor, 1971; Ajmera and Toor, 1976). [In those studies, PDF was assumed to be Gaussian. In essence, what was measured was the variance of the PDF, although Shenoy and Toor (1989) applied the IR method in the

sense used here to extract the actual PDF's from the Vassilatos and Mao data.]

In the CI method (Shenoy, 1988; Shenoy and Toor, 1988), the local time mean indicator color intensity is measured with a fiber optic light probe, a method which conveniently provides three-dimensional spatial resolution. In both methods the reactant feed concentration ratio is varied. If the appropriate concentration measures are chosen, then with the CI method, ideally the *first* derivative of the color density with respect to feed concentration ratio is the PDF, and in the IR method the *second* derivative of the reactant concentration with respect to feed concentration ratio is the PDF. Both methods give the variance of the PDF from a single measurement if the shape of the PDF is known, and both also allow determination of the variance *without* differentiation or knowledge of the shape of the PDF.

The two methods are obviously closely related. They will be reviewed briefly before the relationship between them is developed.

## Theory Common to Both Methods

If two mutually soluble fluids are mixed, one containing  $C_{A0}$  moles of  $A$  per unit volume and one containing  $C_{B0}$  moles of  $B$  per unit volume and the reaction,  $A + nB \rightleftharpoons \text{Product}$ , takes place, then under certain commonly attainable conditions the instantaneous local concentrations of  $A$  and  $B$  are related by (Shenoy and Toor, 1989)

$$W_A - W_B = f - u. \quad (1)$$

The concentration measures,  $W_A$  and  $W_B$ , are defined by

$$W_A = \frac{nC_A}{nC_{AO} + C_{BO}}, \quad (1a)$$

$$W_B = \frac{C_B}{nC_{AO} + C_{BO}} \quad (1b)$$

as  $u$  is defined as

$$u = \frac{W_{BO}}{W_{AO} + W_{BO}} = \frac{C_{BO}}{nC_{AO} + C_{BO}} \quad (1c)$$

while  $f$  is the dimensionless concentration of  $A$  when  $B$  is not present; hence,  $f$  is the passive tracer concentration whose behavior describes the *mixing alone*.

Equation 1 can be derived in the manner of Danckwerts (1957) and Shenoy and Toor (1988) by mixing a fraction,  $f$ , of the  $A$  stream with a fraction,  $1-f$ , of the  $B$  stream. But the more useful interpretation of  $f$  as the dimensionless concentration of a nonreacting tracer is obtained from the convective diffusion equations; for Eq. 1 can also be obtained by applying the Burke and Schumann transformation (which assumes equal reactant diffusivities) (Burke and Schumann, 1928) to the convective diffusion equations (Toor, 1962; Li and Toor, 1986).

Acid-base reactions are effectively instantaneous, so local equilibrium exists. Hence, for strong acids and bases,  $W_A$  and  $W_B$  are related by

$$W_A W_B = \frac{nK_w}{(nC_{AO} + C_{BO})^2}. \quad (2)$$

Equations 1 and 2 together give  $W_A$  and  $W_B$  as a function of  $f$ . It is this relationship which is the basis for both of the methods under discussion.

### Instantaneous Reaction Method

For concentrations of practical interest ( $10^{-2}$ – $10^{-3}$   $N$  acids and bases), the right-hand side of Eq. 2 is small enough for the reaction to be considered irreversible. Then, since  $W_A$  and  $W_B$  are nonnegative, Eq. 1 gives

$$W_B = 0 \quad \text{and} \quad W_A = f - u \quad \text{for} \quad f > u \quad (3a)$$

and

$$W_A = 0 \quad \text{and} \quad W_B = u - f \quad \text{for} \quad f < u. \quad (3b)$$

As  $W_A$  and  $W_B$  are functions of  $f$  and  $u$  only, the mean concentrations are given by

$$\begin{aligned} \bar{W}_A(u) &= \int_0^1 W_A(f, u) \phi(f) df \\ &= \int_u^1 (f - u) \phi(f) df \quad (4a) \end{aligned}$$

and

$$\begin{aligned} \bar{W}_B(u) &= \int_0^1 W_B(f, u) \phi(f) df \\ &= \int_0^u (u - f) \phi(f) df \quad (4b) \end{aligned}$$

where  $\phi(f)$  is the PDF of the instantaneous dimensionless tracer concentration,  $f$ . Differentiating the above expressions with respect to  $u$  at a fixed point then gives the cumulative probability distribution functions on a "more than (the lower limit)" and a "less than (the upper limit)" basis (Shenoy and Toor, 1989). Thus,

$$\int_u^1 \phi(f) df = -d\bar{W}_A/du \quad (5a)$$

and

$$\int_0^u \phi(f) df = d\bar{W}_B/du. \quad (5b)$$

Differentiating once again gives the PDF as the second derivative of  $\bar{W}_A$  or  $\bar{W}_B$  (Kappel, 1979; Shenoy and Toor, 1989). Thus, in this method, differentiating the measured mean reactant concentration a second time gives the PDF. The variance can then be obtained from the PDF, but can also be obtained from the expression which follows from the earlier equations (Shenoy and Toor, 1989)

$$\sigma^2 = 2 \int_0^1 \bar{W}_A du - (\bar{f})^2 = 2 \int_0^1 \bar{W}_B du - (1 - \bar{f})^2. \quad (6)$$

Figures 1 and 2 from Shenoy and Toor (1989) show the geometrical significance of Eq. 6.

If the PDF is Gaussian and the tails are neglected, Eq. 4a gives

$$\bar{W}_A = \frac{\sigma}{\sqrt{2}} \text{ierfc} \left( \frac{u - \bar{f}}{\sqrt{2}\sigma} \right) \quad (7)$$

so under this circumstance, one measurement of  $\bar{W}_A$  yields the variance.

### Chemical Indicator Method

In this method, rather than following the acid-base reaction itself, one follows the color intensity of an indicator which is present and whose equilibrium is shifted by the acid-base reaction. Equations 1 and 2 still hold, to which is appended the equation which relates the reactant concentrations (actually  $H^+$  and

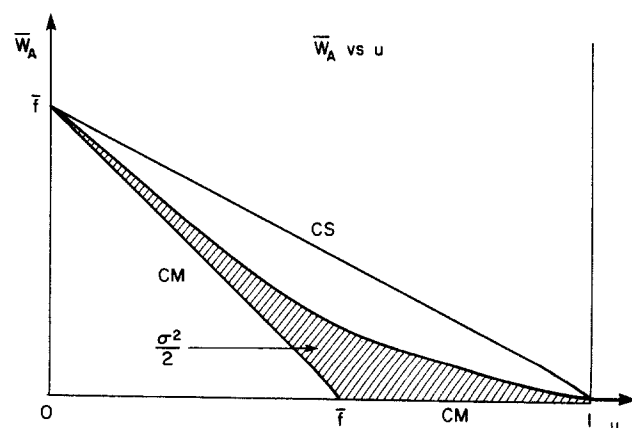
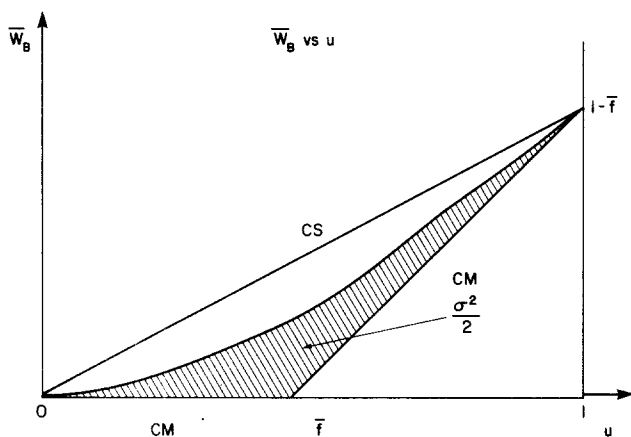


Figure 1. Typical reactive mixing plot in terms of species A.



**Figure 2. Typical reactive mixing plot in terms of species B.**

$\text{OH}^-$ ) to the indicator color (Li and Toor, 1986; Shenoy, 1988)

$$X_I = \frac{1}{1 + K_w/C_A K_I} \quad (8)$$

Equation 8 assumes equal diffusivities of both forms of the indicator. It applies only if the indicator concentration is the same in both streams—otherwise other forms hold (Shenoy, 1988). Equations 1, 2 and 8 relate  $X_I$  to  $f$  so the mean color intensity is given by

$$\bar{X}_I(u) = \int_0^1 X_I(f, u) \phi(f) df. \quad (9)$$

An ideal indicator (and bromothymol blue can be close enough) (Shenoy, 1988) is totally in its acid form for  $\text{pH} < 7$  and totally in its basic form for  $\text{pH} > 7$ . For such an indicator, Eqs. 1, 2 and 8 show that  $X_I(f, u)$  makes a step change from 0 to 1 at  $f = u$ , so Eq. 9 becomes

$$\bar{X}_I(u) = \int_u^1 \phi(f) df \quad (10)$$

and the derivative of this equation is

$$-\frac{d\bar{X}_I(u)}{du} = \phi(u). \quad (11)$$

Thus, in this method, differentiating  $\bar{X}_I(u)$  once only gives the PDF. As before, an equation analogous to Eq. 6 gives the variance directly from measured quantities (Hartung and Hiby, 1971; Shenoy and Toor, 1988)

$$\sigma^2 = 2 \int_0^1 \bar{X}_I(u) u du - (\bar{f})^2 \quad (12)$$

and one analogous to Eq. 7 holds if the PDF is Gaussian (Shenoy and Toor, 1989)

$$\bar{X}_I = \frac{1}{2} \text{erfc} \left( \frac{u - \bar{f}}{\sqrt{2}\sigma} \right). \quad (13)$$

Again the tails have been neglected.

## Relationship Between the Two Methods

It is clear from the previous discussion that the IR and CI methods are closely related and a combination of Eqs. 5a and 10 gives the explicit relationship,

$$\frac{d\bar{W}_A(u)}{du} = -\bar{X}_I(u). \quad (14a)$$

Another form, obtained by integrating with  $\bar{W}_A(1) = 0$  is

$$\bar{W}_A(u) = \int_u^1 \bar{X}_I(u') du'. \quad (15a)$$

The  $B$  forms are

$$\frac{d\bar{W}_B(u)}{du} = 1 - \bar{X}_I(u) \quad (14b)$$

$$\bar{W}_B(u) = u - \int_0^u \bar{X}_I(u') du'. \quad (15b)$$

Since  $\bar{W}_A(0) = \bar{f}$ , Eq. 15a gives

$$\bar{f} = \int_0^1 \bar{X}_I(u) du. \quad (16)$$

Thus, the integral of the PDF gives the mean color density,  $\bar{X}_I(u)$ , and the mean color density plot of the indicator method, as per Eq. 10; and the integral of the mean color density gives  $\bar{W}_A(u)$ , as per Eq. 15a, and the reactive mixing plot of the instantaneous reaction method. As a corollary, differentiation of the mean color density gives the PDF according to Eq. 11, and integration gives the reactant concentration according to Eq. 15a. This is shown in Figure 3, which provides the unified picture for the PDF, the mean color density plot, and the reactive mixing plot (each corresponds to a different row) at a particular location in a turbulent system for four different states of mixing (each corresponding to a different column). The limiting cases of complete segregation (CS) and complete mixing (CM) are shown along with two intermediate states of mixing (one where the original Dirac deltas in the PDF have completely vanished, i.e., no virgin fluid from either of the two feed streams is present at the point of interest, and the other where the Dirac deltas are yet to disappear). Starting with the middle row, integration takes  $\bar{X}_I(u)$  up to  $\bar{W}_A(u)$  and differentiation takes it down to  $\phi(f)$ . This is demonstrated in the following sections with measured values of  $\bar{X}_I(u)$ .

## Measurement of $\bar{X}_I(u)$

A fiber optic light probe with a gap width of about 2 mm and a fiber optic bundle diameter of approximately 0.7 mm was utilized to measure the local time-averaged indicator color density in reacting and nonreacting experiments, where the behavior of an axisymmetric turbulent jet mixing into a very large, stagnant tank was investigated. In the reacting experiments, dilute NaOH was in the jet and dilute HCl in the ambient fluid, and both the jet and surrounding environment contained a chemical indicator at the same concentration. In the nonreacting experiments (used to measure  $\bar{f}$ ), the jet contained a chemical indi-

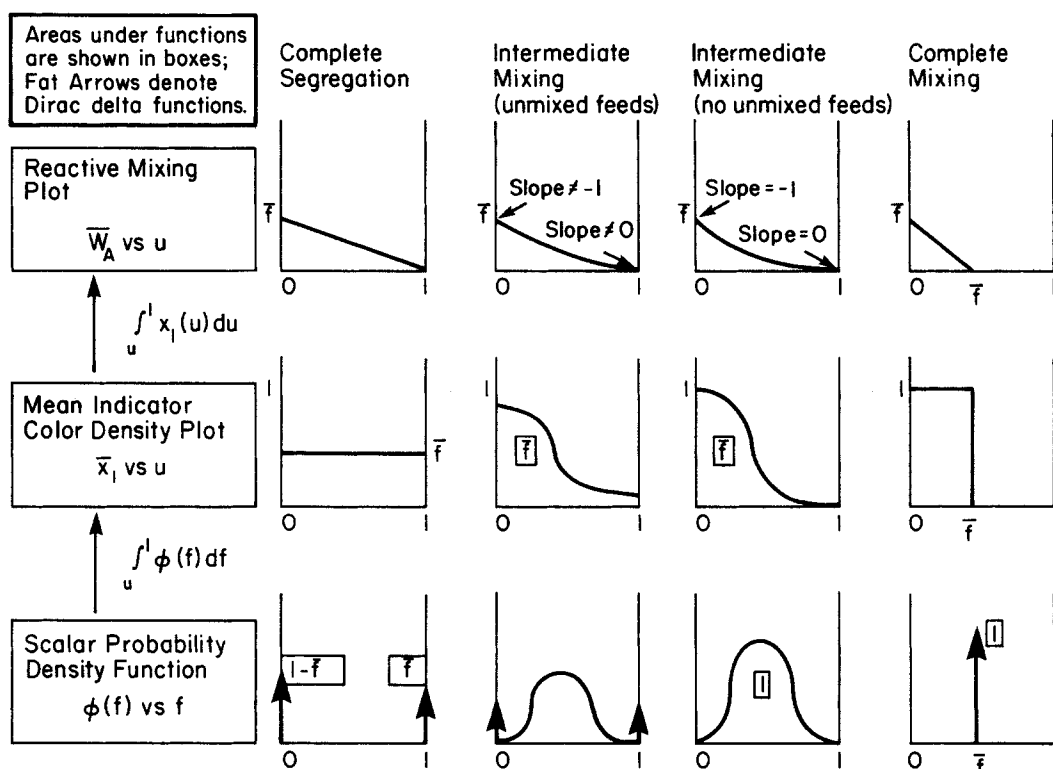


Figure 3. Unified picture: PDF profiles, mean color density plots, and reactive mixing plots for four different states of mixing.

cator (which acted like an inert tracer) and both the jet and ambient fluid contained NaOH at the same concentration. All the experimental measurements are for a circular jet of nozzle diameter,  $d = 0.003175$  m, at a jet Reynolds number of 9,000. Details of the experiments are available elsewhere (Shenoy, 1988; Shenoy and Toor, 1988).

Two chemical indicators were examined: phenolphthalein was chosen because it is a one-color indicator, while bromothymol blue was selected because its color transition is almost symmetrical around the neutral point. Phenolphthalein experiments (Shenoy and Toor, 1988) will not be discussed here as the color transition is far from sharp and the data requires correction to account for the finite color transition region. However, bromothymol blue, with an alkaline feed of pH 11.4, shows a very sharp color transition (Figure 4). Even with  $\text{CO}_2$  absorbed from the air, which smears the transition somewhat, the perfectly sharp approximation appears to be valid, so the earlier equations are used to analyze the data without correction.

### The Mean Indicator Color Density Plot

Figure 5 shows mean indicator color density plots  $[\bar{X}_i(u)]$  at axial distances,  $z$ , of 15 and 20 jet dia. downstream on the centerline. The experiments were conducted with an alkaline feed of initial pH, 11.4 ( $C_{AO} = 0.025$  N) and with 30 mg/L of bromothymol blue. Each measurement was made over a 3 min. period which was short enough to permit the bulk concentration in the tank to be assumed constant. The curve was generated by starting at  $u = 0$  (very dilute acid in the large tank) and progressively increasing  $u$  toward 1 by increasing the tank acidity after each

data point measurement. A cubic spline smoothing routine was used to obtain the solid lines in Figure 5. Then Eqs. 12 and 16, on numerically integrating, give

$$\bar{f} = 0.362 \quad \text{and} \quad \sigma = 0.096 \quad \text{at} \quad z/d = 15$$

$$\bar{f} = 0.298 \quad \text{and} \quad \sigma = 0.069 \quad \text{at} \quad z/d = 20$$

The above values of  $\bar{f}$  are in good agreement with those obtained directly by nonreacting experiments (namely,  $\bar{f} = 0.368$  at  $z/d = 15$ , and  $\bar{f} = 0.305$  at  $z/d = 20$ ) (Shenoy, 1988).

The  $\bar{X}_i$  vs.  $u$  data, when directly plotted on probability paper (Figure 6) utilizing Eq. 10, fall approximately on straight lines suggesting that the Gaussian assumption for the PDF is reasonable at these locations. The scalar PDF profiles are next obtained by differentiating the cubic spline fits in Figure 5 and changing the sign. Though the areas under the PDF obtained on numerical integration check to approximately unity, the PDF's shown in Figure 7 for the earlier positions reflect the unstable nature of the numerical differentiation operation.

Since the normal distribution appears to be a reasonable assumption according to Figure 6, each individual measurement of  $\bar{X}_i$  has been used to estimate  $\sigma$  from Eq. 13, giving

$$\sigma = 0.087 \pm 0.013 \quad (\text{using 17 data points}) \quad \text{at} \quad z/d = 15$$

$$\sigma = 0.075 \pm 0.010 \quad (\text{using 14 data points}) \quad \text{at} \quad z/d = 20$$

These results, on considering the error bands, are in agreement with the earlier values of  $\sigma$  computed by Eq. 12 without assuming a PDF.

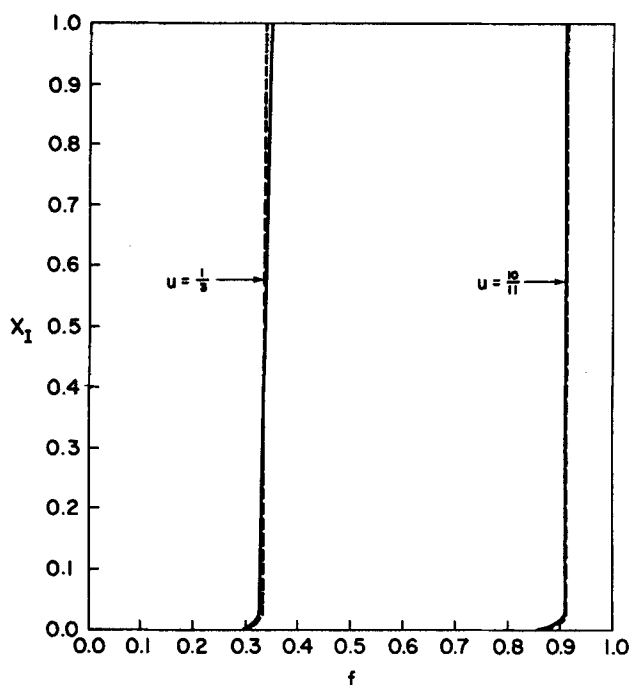


**Figure 4. Instantaneous color density for bromothymol blue from Eqs. 1, 2 and 8.**

—  $C_{A0} = 0.0025 N_1$ , ---  $C_{A0} = 0.025 N_1$

#### From Mean Color Density Plot to Reactive Mixing Plot

In this section, Eq. 15 is used to generate the reactive mixing plots at the jet centerline by numerical integration of the data in Figure 5. Such plots for  $\bar{W}_A$  vs.  $u$  and  $\bar{W}_B$  vs.  $u$  are shown in Figure 8, where the solid lines represent the reactive mixing curves at  $z/d = 15$ , while the dashed ones at  $z/d = 20$ . Each individual curve exhibits the features already discussed by Shenoy and

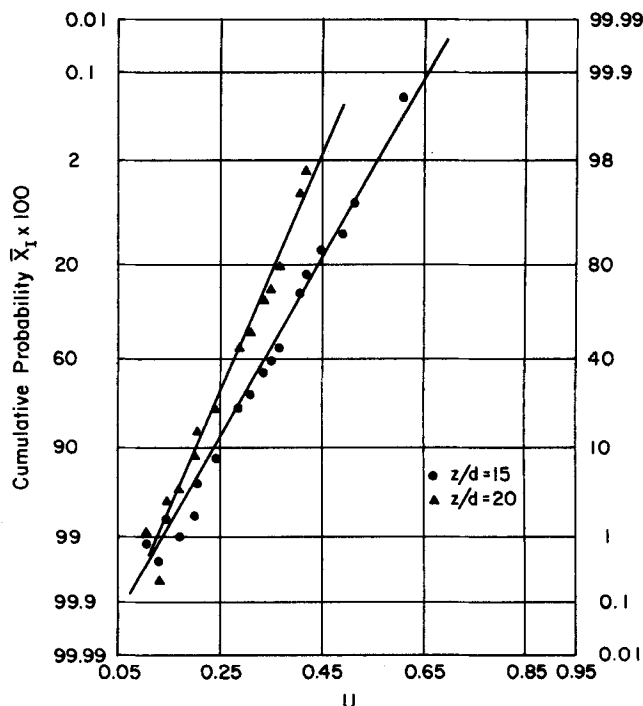


**Figure 6. Probability plot for normal distribution.**

Toor (1989) with regard to the intercepts and limiting behavior on reactive mixing plots.

When compared with the reactive mixing plots for the data of Vassilatos and Toor (1965) and Mao and Toor (1971) which were for *one-dimensional* systems and were analyzed by Shenoy and Toor (1989), Figure 8 shows some new features. These are:

- In this two-dimensional system, the value of  $\bar{f}$  changes with distance downstream and this is noticeable in the changing intercepts on the ordinate of Figure 8.

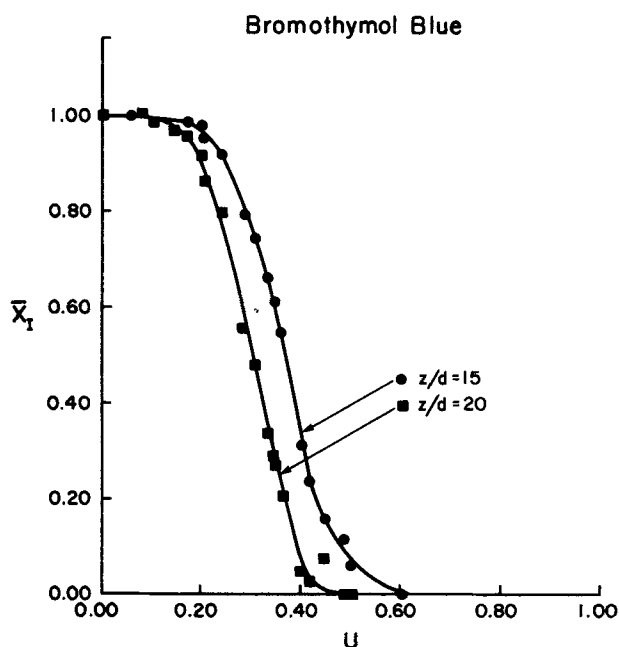


**Figure 5. Measured mean color density**

15, 20 jet dia. downstream, on jet centerline;  $Re = 9,000$ .

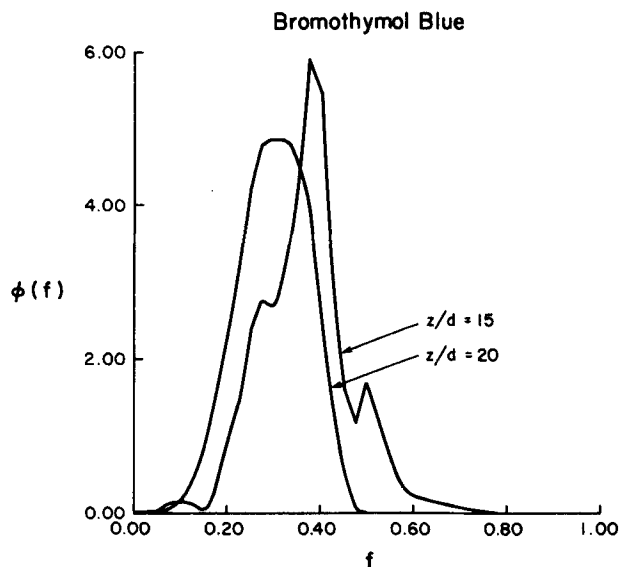


**Figure 7. Scalar PDF profiles.**

$Re = 9,000$ ; 15, 20 jet dia. downstream on centerline; PDF areas: 1.0000 ( $z/d = 15$ ); 1.0005 ( $z/d = 20$ ).

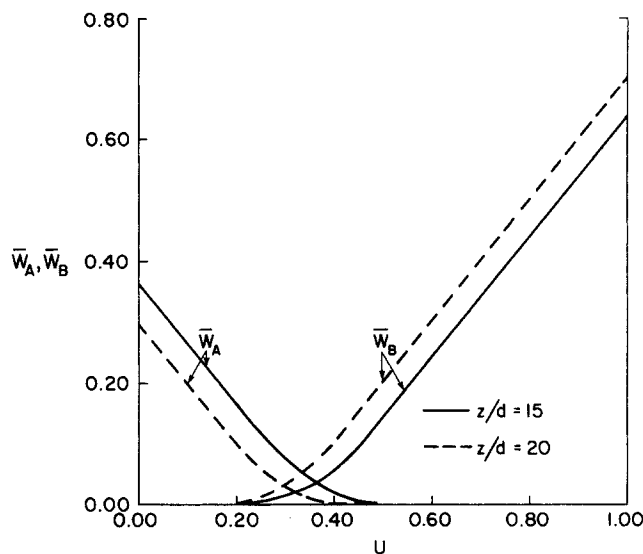


**Figure 8. Reactive mixing plots from mean color density data (bromothymol blue).**  
 $z/d = 15, 20$  on jet centerline.

• As in a one-dimensional system, the limiting behavior of “complete segregation” and “complete mixing” exists in the form of asymptotes on the reactive mixing plot. The asymptotes, which are piecewise linear, are not actually drawn in Figure 8 to prevent clutter; however, the asymptotes can be visualized by referring to Figures 1 and 2. The major difference is that, in the one-dimensional reactor, these are actually observable in the system (i.e., complete segregation at the inlet and complete mixing far downstream). On the other hand, for two- and three-dimensional reactors, these are hypothetical cases where the two limits correspond to the reactive mixing curves *if the reactants had been completely segregated or completely mixed at that point*. This implies that  $\bar{f}$  is at the given value, but the variance is given by  $\bar{f}(1 - \bar{f})$  and zero for the “complete segregation” and “complete mixing” cases, respectively.

• Even though they correspond to hypothetical situations, these asymptotes, especially the completely mixed ones, give a geometrical significance to the variance through Eq. 6—the variance is twice the area between the reactive mixing curve and the completely mixed asymptote—in accord with the intuitive idea that the variance is a measure of the deviation from the completely mixed state.

## Acknowledgment

This work was supported by a National Science Foundation Grant No. CBT-8505378.

## Notation

$A$  = reactant (typically alkaline)  
 $B$  = reactant (typically acid)  
 $C$  = concentration, mol/L  
 $CM$  = “complete mixing” limit  
 $CS$  = “complete segregation” limit

$d$  = jet nozzle diameter  
 $\text{erfc}(x)$  = complementary error function of  $(x)$   
 $f$  = dimensionless concentration of nonreacting tracer  
 $\text{ierfc}(x) = \int_x^\infty \text{erfc}(x') dx'$   
 $K_I$  = dissociation constant of indicator  
 $K_w$  = ion product of water,  $10^{-14}$  (mol/L)<sup>2</sup> at ambient conditions  
 $n$  = stoichiometric coefficient  
 $u$  = defined in Eq. 1c  
 $W_A, W_B$  = dimensionless reactant concentrations as defined in Eqs. 1a and 1b  
 $X_I$  = fraction of the base form of indicator or “absorbing color” density  
 $z$  = axial distance downstream

## Greek letters

$\phi$  = probability density function (PDF) of the nonreacting tracer  
 $\sigma^2$  = variance of the PDF

## Subscripts

$A, B, I$  = reacting species  
 $0$  = value in feed streams

## Superscripts

— = time-averaged (or space-averaged)

## Literature Cited

- Ajmera, P. J., and H. L. Toor, “Reactive Mixing in Turbulent Gases,” *Chem. Eng. Comm.*, **2**, 115 (1976).
- Burke, S. P., and T. E. W. Schumann, “Diffusion Flames,” *Ind. Eng. Chem.*, **20**, 998 (1928).
- Danckwerts, P. V., “Measurement of Molecular Homogeneity in a Mixture,” *Chem. Eng. Sci.*, **7**, 116 (1957).
- Hartung, K. H., and J. W. Hiby, “A Method for the Evaluation of the Intensity of Segregation,” *Chem. Eng. Sci.*, **26**, 488 (1971).
- Kappel, M., “Development and Application of a Method for Measuring the Mixture Quality of Miscible Liquids: I. State of Research and Theoretical Principles,” *Int. Chem. Eng.*, **19**, 196 (1979).
- Koochesfahani, M. M., and P. E. Dimotakis, “Mixing and Chemical Reactions in a Turbulent Liquid Mixing Layer,” *J. Fluid Mech.*, **170**, 83 (1986).
- Li, K. T., and H. L. Toor, “Chemical Indicators as Mixing Probes. A Possible Way to Measure Micromixing Simply,” *I & EC Fund.*, **25**, 719 (1986).
- Mao, K. W., and H. L. Toor, “Second-Order Chemical Reactions with Turbulent Mixing,” *I & EC Fund.*, **10**, 192 (1971).
- Shenoy, U. V., “The Development of a Chemical Indicator Probe Method for Measuring Turbulent Micromixing,” PhD Thesis, Carnegie Mellon University (1988).
- Shenoy, U. V., and H. L. Toor, “Micromixing Measurements with Chemical Indicators,” *Proc. 6th Eur. Conf. on Mixing*, Pavia, Italy (1988).
- Shenoy, U. V., and H. L. Toor, “Turbulent Micromixing Parameters from Reactive Mixing Measurements,” *AIChE J.*, **35**, 1692 (1989).
- Toor, H. L., “Mass Transfer in Dilute Turbulent and Nonturbulent Systems with Rapid Irreversible Reactions and Equal Diffusivities,” *AIChE J.*, **8**, 70 (1962).
- Vassiliatos, G., and H. L. Toor, “Second-Order Chemical Reactions in a Homogeneous Turbulent Field,” *AIChE J.*, **11**, 666 (1965).

Manuscript received July 12, 1989, and revision received Nov. 27, 1989.